Saharan dust deposition in the Carpathian Basin and its possible effects on interglacial soil formation

György Varga1,*; Csaba Cserháti2; János Kovács3,4; Zoltán Szalai1,5

1Geographical Institute, Research Centre for Astronomy and Earth Sciences, Hungarian Academy of Sciences, Budaörsi út 45, H-1112 Budapest, Hungary

2Department of Solid State Physics, University of Debrecen, Bem tér 18/b, H-4026 Debrecen, Hungary

3Department of Geology & Meteorology, University of Pécs, Ifjúság u. 6, H-7624 Pécs, Hungary

4Environmental Analytical & Geoanalytical Research Group, Szentágothai Research Centre, University of Pécs, Ifjúság u. 20, H-7624 Pécs, Hungary

5Department of Environmental and Landscape Geography (Institute of Geography and Earth Sciences, Faculty of Science), Eötvös University, Pázmány Péter sétány 1/c, H-1117 Budapest, Hungary

*Corresponding author (E-mail: varga.gyorgy@csfk.mta.hu)

Abstract

Several hundred tons of windblown dust material are lifted into the atmosphere and are transported every year from Saharan dust source areas towards Europe having an important climatic and other environmental effect also on distant areas. According to the systematic observations of modern Saharan dust events, it can be stated that dust deflated from North

African source areas is a significant constituent of the atmosphere of the Carpathian Basin and Saharan dust deposition events are identifiable several times in a year. Dust episodes are connected to distinct meteorological situations, which are also the determining factors of the different kinds of depositional mechanisms. By using the adjusted values of dust deposition simulations of numerical models, the annual Saharan dust flux can be set into the range of 3.2 to 5.4 g/m^2/y.

Based on the results of past mass accumulation rates calculated from stratigraphic and sedimentary data of loess-paleosol sequences, the relative contribution of Saharan dust to interglacial paleosol material was quantified. According to these calculations, North African exotic dust material can represent 20-30% of clay and fine silt-sized soil components of interglacial paleosols in the Carpathian Basin. The syngenetic contribution of external aeolian dust material is capable to modify physicochemical properties of soils and hereby the paleoclimatic interpretation of these pedogene stratigraphic units.

Highlights:

Saharan dust events have been frequent in the Carpathian Basin also during interglacial periods

Annual Saharan dust flux can be set into the range of 3.2 to 5.4 g/m^2/y

Admixture of Saharan dust material has a major influence on soil-formation

Saharan dust material can represent 20-30% of clay and fine silt-sized soil components of interglacial paleosols in the Carpathian Basin

Keywords: Saharan dust; Carpathian Basin; Pleistocene interglacial; dust flux

1. Introduction

The study of aeolian dust and dust storms is an area of growing interest and importance in Earth and atmospheric science communities. Huge amount of mineral dust particles (which diameters range from several hundred nanometres to ~100 μm) is emitted from arid and semiarid areas. The most intense and active dust source areas are located in North Africa accounting for the 50-70% of global mineral dust emission (Goudie and Middleton, 2001). Several hundred tons of windblown dust material are lifted into the atmosphere every year and are transported northward from Saharan source areas into direction of Europe (Moulin et al., 1998; Stuut et al., 2009). Recently, a considerable number of studies have grown up around the subject of direct and indirect climatic effects of mineral dust even at areas situating relatively far from the sources (Harrison et al., 2001; Kohfeld and Tegen, 2007; Maher et al., 2010). Dust particles are capable to absorb, scatter and reflect the incoming shortwave and outgoing longwave radiation and have also an effect on the overall planetary energy balance by changing the surface albedo. Additionally, dust storms transport important nutrients to seas and oceans enhancing the primary phytoplankton production and influencing the uptake of atmospheric CO_2.

Beside several other environmental effects, aeolian dust plays also an important geological role as parent material of aeolian dust deposits (e.g. loess-paleosol series, windblown material in deep sea sediments, dust layers in ice cores) (Pye, 1987, 1995). These records of mineral dust deposition indicate that the amount of atmospheric windblown dust was several orders of magnitude higher in certain periods. Activity of source areas, amount of emitted mineral dust, as well as frequency and magnitude of Saharan dust intrusions into Europe are showing a wide diversity, indicating that even moderate climatic fluctuations are causing significant changes in the dust budget. In general, Pleistocene glacials were accompanied by high dust emissions from major source areas due to the interactions of main controlling mechanisms (e.g. availability of loose fine-grained material, land surface characteristics, wind speed and gustiness caused by more steepened meridional temperature gradients). Mediterranean marine sediments and terrestrial sequences of PeriSaharan desert loess deposits suggest also an enhanced dust deposition from Saharan sources during Pleistocene cold periods (Yaalon and Dan, 1974; Tsoar and Pye, 1987). The increased North African dust emission was caused by the more uneven annual distribution of rainfall, gustier winds and more intense cyclogenesis caused by more frequent penetration of cold Arctic air-masses.

During interglacials, the Saharan dust emission was reduced compared to glacials. However, significant role of Saharan dust addition in interglacial soil formation has been reported from several sites around the Mediterranean: MacLeod (1980) used grain size analyses to support the windblown origin of pedogene units in Greece; Durn et al. (1999) and later Durn (2003) concluded that red soils in Croatia was developed from previously deposited dust material based on clay minerals and geochemical indicators; Genova et al. (2001) investigated terra rossa in Sardinia to infer an aeolian origin, while Jackson et al. (1982) identified Saharan dust as parent material of soils in Italy, as did Jahn et al. (1991) in Portugal, Nihlén and Olsson (1995) in Crete and Atalay (1997) in Turkey. According to the immobile trace element analyses of Muhs et al. (2010) in Majorca, the addition of Saharan dust was a dominant factor in the formation of soils in the area. Jordanova et al. (2013) studied relict reddish pedogene units in Bulgaria and their measurements of trace and rare element content and magnetic data suggested a North African aeolian contribution during the soil formation.

The windblown origin of certain types of widespread red Mediterranean soils has been a matter of debate for ca. hundred years (Leiningen, 1915, 1930). Rapp (1983) stated that the development of terra rossa soils in south Europe is not a result of the residual weathering of the bedrock, but the parent material of soils might be originated from the Sahara. At several places, the residuum origin from the underlying (mainly limestone) bedrock is not probable. The unrealistic amounts of required carbonate rock dissolution, mineralogical issues, quartz-rich soils on carbonate-rich, quartz-free bedrocks cannot be explained by the 'residue theory' of these units. Addition of aeolian dust particles as an enrichment was proposed by Kubiëna (1953) and this theory was later developed by Yaalon and Ganor (1973), and Yaalon (1997). The term 'aeolian contamination' was introduced also by Yaalon and Ganor (1973), to describe soil property changing modifications made by aeolian increments. Identification of external aeolian dust material in soils is a challenging problem, however, nowadays, the role of aeolian dust as parent material of soils and soils with different degrees of aeolian influence has been known from several locations in the Mediterranean, as well as in other parts of the world.

In spite of the more intense glacial North African dust emission, the recognition of Saharan dust material in Central European loess-paleosol sequences regarded as ones of the most important climate archives has remained a challenging problem. According to a simplified model of aeolian dust sedimentation, dust accumulation is a result of local, dust storm-related coarse-grained (30< μm: middle- and coarse-silt fraction with a casual presence of very fine-sand (<~100 μm)) dust deposition and an additional incorporation of fine-grained background dust load (<20-30 μm: clay, fine-silt fraction). The source of the coarse-grained sub-population is local material, deflated from loosely consolidated Upper Miocene and Lower Pliocene deposits eroded from the Alps and Carpathians, from floodplain deposits and from the deposits of the former Lake Pannon (Kovács et al., 2008, 2011; Bokhorst et al., 2011). At the same time, the origin of fine-grained component is primarily the result of deposition of dust particles from distant sources, and partly post-depositional alteration and disintegration of aggregates (Bokhorst et al., 2011). Present-day far-travelled North African dust samples collected in Europe are almost totally composed of clayey and fine-silty material with occasional occurrence of some slightly larger mineral particles. The Pleistocene glacial loess formation was primarily determined by deposition of silty material from local sources, transported by NW winds (Bokhorst et al., 2011), the signals of fine-grained dust addition from distant sources were depleted by the enhanced local dust fluxes.

Local dust accumulation in the Carpathian Basin was terminated during interglacials (Vandenberghe et al., 2014). So far, however, very little attention has been paid to the role of syngenetic external dust accretion to interglacial paleosols in the Carpathian Basin, albeit present-day Saharan dust events have been considerably frequent. It is assumed that the amount of interglacial North African dust deposition was similar to the recent conditions. The interpretation of paleosol records must also take into account possible incorporation of far-travelled dust material from distant sources. This is especially true for the Carpathian Basin, where after the infilling and desiccation of Lake Pannon terrestrial windblown dust accumulation played the most prevailing role in sedimentation.

This paper is aimed at providing (1) a complex review of the frequency, synoptic background, transportation routes and intensity of present day Saharan dust events and deposition of windblown desert particles in the Carpathian Basin; and (2) an estimate on the past Saharan dust sedimentation and its possible influence on soil properties of past soils (modified by syngenetic, external dust addition) of the Carpathian Basin.

2. Materials and methods

2.1. Investigation area

The Carpathian Basin (CB: 45°–48.5°N, 16°–23°E) is located in Central Europe and its subsiding depression is framed by the Alps, Carpathians and Dinaric mountain ranges. More than half of the area is covered by aeolian dust deposits, mainly the products of Pleistocene glacial loess formation periods (Marković et al., 2011, 2015; Újvári et al., 2014), however, sediments of older dust accumulation intervals have also been preserved as Pliocene (and partly Pleistocene) red clay deposits (Kovács et al., 2011, 2013). The thick aeolian dust deposits of the area provide insight into the cyclic climatic variations of the Quaternary glacial-interglacial periods and are one of the most important terrestrial archives of past climatic changes is Europe. The thick, pale yellow loess deposits are the product of the increased dust flux of cold and dry glacial periods, while during warmer and moister interglacials, soils were formed from the formerly deposited aeolian loess (Varga et al., 2012; Újvári et al., 2014; Vandenberghe et al., 2014).

In this paper, a generalized loess-paleosol sequence is the basis of our calculations, which was set up primarily based on the Paks loess section, situated on the right bank of the River Danube in the mid-Carpathian Basin. The accumulation of the well-known Paks Loess Formation started in the latest part of the Lower Pleistocene and represents a record of approximately the last 1 million years of windblown dust accumulation in the Carpathian Basin (Horváth and Bradák, 2014; Újvári et al., 2014; Marković et al., 2015). The Late and partly, Middle Pleistocene loess deposits are separated by different kinds of interglacial steppe, forest-steppe and brown forest soils, while the older pedogene horizons are rubefied red soils (so-called Paks Double 1 [PD1], Paks Double 2 [PD2] and Paks-Dunakömlőd [PDK] soils (Pécsi, 1990; Bronger, 2003). According to published chronological and stratigraphic data, the units of younger member of the sequence can be correlated with MIS-7 to MIS-11 interglacials. The paleosol units of MIS-5 were missing in the studied sequence, samples were sampled from the Tamási site (Hungary). The MIS-13 and MIS-15 units are not so dominant in the Hungarian sections, only the remnants of two brown forest soils and two pseudogley soils could be located in the Paks loess series.

The chronological subdivision of old paleosols is based on the controversial position of Matuyama-Brunhes Boundary (MIS-19), the only reference point, which was placed in the upper part of the PD2 soil (Sartori et al., 1999). However, the correlation of the thick, well-developed, rubefied PD1 paleosol with MIS-17 interglacial is unlikely. According to the studies of Basarin et al. (2014) and Buggle et al. (2014) MIS-17 is represented by the V-S6 fossil Cambisol in Serbia and its iron mineralogical proxies indicate lower temperature and/or more summer precipitation, an unsuitable condition for rubefied brown forest soil formation. Based on these considerations and a recently proposed Danube loess stratigraphic subdivision by Marković et al. (2015) the older red soils are equivalent to PD1: MIS-19; PD2: MIS-21 and PDK: MIS-25 (Fig.1.).

The Paks Loess Formation is generally underlained by the deposits of the Tengelic Red Clay Formation, which age is Late Pliocene to Early Pleistocene, and is regarded as a thick paleosol complex, a series of B horizons. The lower, older member of this unit is rich in smectite, mixed-layer smectite/kaolinite and kaolinite, and was developed under a humid subtropical climate. The younger member of the red clay unit includes more fresh material (illite, chlorite) and was formed in a warm Mediterranean-like climate (Kovács et al., 2013). Similar deposits are known from other sites of the region: Stari Slankamen – Serbia (Marković et al., 2011); Viatovo – Bulgaria (Jordanova et al., 2008).

2.2. Modern dust

Dust load

The frequency and magnitude of recent Saharan dust episodes in the investigated area were determined by using the daily NASA Aerosol Index (AI) data-matrices (from 1979 to 2012). AI measures of how much the wavelength of backscattered ultraviolet radiation from an atmosphere containing aerosols differs from a pure molecular atmosphere; its positive values indicate absorbing aerosols. For a detailed description of the method, see Varga et al. (2013; 2014a) and references therein.

Mean geopotential height (at 700 mb), vector wind and meridional flow data of the identified episodes were obtained from the NCEP/NCAR Reanalysis project (Kalnay et al., 1996) and backward trajectory calculations were made with the NOAA HYSPLIT model (Draxler and Hess, 1997; Draxler and Rolph, 2012) to distinguish different kinds of meteorological conditions responsible for dust transportation.

Dust deposition

In contrast to dust load, there is much less information about dust deposition. Calculations were made by using the data of BSC-DREAM8b (Barcelona Supercomputing Center's Dust REgional Atmospheric Model) v1.0 and v2.0 dust models and mineral dust model database. Simulation results of the BSC-DREAM8b v1.0 are available from 1 January 2000 to 31 December 2012, while the results of the updated v2.0 calculations are ready for the period between 1 January 2006 and 31 December 2014. The BSC-DREAM8b models predict the atmospheric residence of the eroded fine-grained aeolian material by solving Euler-type partial differential non-linear equations. The meteorological fields are initialized every 24h, while the boundary conditions are updated every 6h (Pérez et al., 2006a, 2006b; Basart et al., 2012). The values in the BSC Mineral Dust Database do not correspond with the daily forecasts; they have been rerun in order to provide long-term homogeneous simulations for the period between 2000 and 2014. The modelled values were compared with the results of the few direct surface observations of published European measurement campaigns (mainly from the Mediterranean).

Particle characteristics of Saharan dust material in the Carpathian Basin

Dust material from five intense Saharan dust deposition events was collected from Hungarian sites (Debrecen, Veszprém and Budapest). Granulometric properties of recently deposited dust samples were determined by using a Hitachi S-4300 CFE scanning electron microscope (SEM), Malvern Morphologi G3-ID automated image analyser and Malvern Mastersizer 3000 (Hydro LV) laser particle size analyser.

2.3. Past dust

Aeolian dust deposits

Widespread aeolian dust deposits enable us to get a proper picture on past aeolian sedimentation. By using published stratigraphic data of sedimentary sequences (Pécsi and Schweitzer, 1995; Gábris, 2007; Újvári et al., 2014) tuned to the compiled global time-frame, past windblown dust accumulation rates were calculated for the investigated area. Based on the detailed stratigraphic and granulometric analyses of red clay-loess-paleosol series, (Plio-) Pleistocene aeolian sedimentation mechanisms of the Carpathian Basin was investigated in detail.

Grain size analyses

Beside the few hundred dust flux and dust concentration calculations obtained from our previous works (Varga et al., 2012), several new samples were collected. The particle size of all sedimentary samples was determined after chemical treatment by adapting the procedure of Konert and Vandenberghe (1997). After treating the samples with (10 ml, 30%) H_2O_2 to oxidize the organic material and (10 ml, 10%) HCl to remove the carbonate, in order to disperse the particles 10 ml of 3.6% $Na_4P_2O_7 \cdot 10H_2O$ was added to the samples. The measurements were made on a Malvern Mastersizer 3000 (Hydro LV) laser diffractometer. Not only size, but also shape parameters of particles are holding vital information on sedimentary mechanisms (transport and deposition) and post-depositional, environment-related alterations. Automated imaging was applied using Malvern Morphologi G3-ID which provides a unique technique to gather direct information on particle size and shape parameters.

Sediment populations

Previous studies on Hungarian loess units (Varga, 2011; Varga et al., 2012; Novothny et al., 2011) unveiled that the particle size distribution curves of aeolian dust deposits are bimodal, with a dominant peak in the middle and coarse silt population and a secondary one in the clay-, fine silt fraction. These characteristics have been found common to formerly analysed aeolian dust deposits in Hungary such as Lower and Middle Pleistocene loess–paleosol and Pliocene–Lower Pleistocene red clays (Kovács, 2008; Kovács et al., 2008, 2011; Varga, 2011) and also to other globally investigated terrestrial wind-blown sediments (e.g. Sun et al. 2004;

Prins et al., 2007; Vriend et al., 2011; Vandenberghe, 2013; Vandenberghe et al., 2014). The bimodal pattern of grain size distribution curves represents the mixing of sediment populations that can be separated from each other by using mathematical methods. According to a simplified model of aeolian dust sedimentation, dust accumulation is a result of local, dust storm-related coarse-grained dust deposition and an additional incorporation of fine-grained background dust load. These two main sedimentary subpopulations are restored in the bimodal particle size distribution curves and can be decomposed by employing mathematical-statistical methods of parametric curve-fitting deconvolution and the EMMA end-member modelling algorithms (Weltje, 1997; Sun et al., 2004; Vriend and Prins, 2005; Weltje and Prins, 2005; Bokhorst et al., 2011; Varga et al., 2012). In this paper, the parametric curve-fitting method was used to decompose the bimodal grain size distribution curves as this technique can be applied for single samples, while EMMA is based on the simultaneous analysis of a whole sequence based on the covariance structure of the dataset. According to the applied technique the bimodal particle size curves can be interpreted as the sum of two overlapping Weibull-functions which represent the two sediment populations. Location, shape and weighting parameters of the two Weibull-functions were modified by an iterative numerical method as a least-square problem to assess the appropriate goodness of fit of the measured and calculated data (Varga et al., 2012).

3. Results and Discussion

3.1. Recent observations of Saharan dust in the Carpathian Basin

Present-day aeolian dust accumulation in the Carpathian Basin is primarily the result of fine-grained dust deposition as the emission from local sources has been ceased. Saharan dust

events are responsible for the dust transportation into Central Europe and these are commonly occurring in spring and summer (Varga et al., 2013). According to the satellite data-based Aerosol Index analyses, three different kinds of meteorological conditions are responsible for these events. During Type-1 situations the south-westerly winds are generated by a southward moving trough (emanated from the direction of Bay of Biscay to NW Africa) and the anticyclonal flow of the divided high-pressure belt. These events are most common in summer as a consequence of thermal convective activity (which creates a permanent reservoir of dust above the Sahara – Israelevich et al., 2002) and the northward migration of subtropical high pressure belt, which is responsible for the formation of steep pressure gradient at the foreside of the atmospheric trough. The higher southerly amplitude of the upper-air trough often leads to cut-off low formation as it becomes a closed circulation, which could generate more intense dust storms in NW Africa and more mineral particles in the atmosphere.
Type-2 meridional winds are connected to southerly warm-sector flow of early springtime low-pressure systems moving eastwards; these are typically mid-latitude Mediterranean cyclones and 'Sharav' cyclones (shallow low-pressure systems developed at the southern side of the Atlas Mts. generated by the temperature difference of the cold sea and the heated continental terrain). The strong meridional flow at front of low-systems transports the mineral dust, which often removes in the Carpathian Basin and at the Balkan Peninsula by wet depositional processes due to strong precipitation activity of Mediterranean cyclones.
Type-3 dust events associated with NW Saharan anticyclonic systems which drift dust towards the higher latitudes and after that westerlies transport the fine-grained material towards the Carpathian Basin. Sometimes, unusually severe and unseasonal dust events are responsible for significant Saharan dust deposition in Central Europe; as it was the situation in 2013 and 2014 (Varga et al., 2014b).

Typical transportation pathways of fine-grained Saharan dust are also associated with these meteorological regimes. The first one and most common synoptic situation contributes to north-eastward dust transportation across the western Mediterranean Sea from salt lakes of high plateau region situated between the Tell Atlas and Saharan Atlas Range. Dust material of events connected to Type-2 situations reach the Carpathian Basin directly from the south, while the least common Type-3 events have the longest dust transportation routes across the eastern Atlantic and western Europe.

Saharan dust in the atmosphere of a given region does not necessarily mean dust deposition there, dust laden air-masses often spread further without significant fallout or outwash episodes. There are very few direct measurements of Saharan dust deposition in Europe. Dust models, however, provide valuable information on dust deposition in Central Europe.

Seasonality patterns of dust deposition are showing a much diverse picture compared to the dust loadings or to above mentioned satellite-based Saharan dust event recognitions. Dust particles are removed either by dry deposition or by wet removal processes. Dry dust deposition events are occurring mainly in spring and summer, and the dry fallout events are primarily determined by the amount of available atmospheric mineral dust, which settles down by turbulent processes and mainly due to gravitational settling. On the contrary, wet dust washout episodes have summer minima and winter maxima (Fig. 2.). BSC DREAM8b v1.0 model simulations for the period between 2000 and 2012 provided an annual mean of 0.0285 $g/m^2/y$ dry and 0.034 $g/m^2/y$ wet deposition values, which is equivalent to a total of 0.0636 $g/m^2/y$. The updated v2.0 version for the period of 2006-2014 gave significantly larger values: 0.133 $g/m^2/y$ dry; 0.085 $g/m^2/y$ wet and 0.219 $g/m^2/y$ total yearly deposition. There is a slight dominance of dry deposition processes over the wet scavenging; the relative ratio of dry and wet removal is ~60% and ~40 %. By comparing the results of the overlapping period between 2006 and 2012 of the v1.0 and v2.0 simulations, the updated depositional scheme of the newer version provided ~3.7-fold values in case of dry deposition and ~1.9-fold increase in results of the wet deposition.

Information available from individual events suggests that the simulated wet and dry dust deposition rates from the Carpathian Basin are significantly underestimated. Several intense dust events have been documented in the near past and fortunately sampling from the deposited material was also possible in these cases. The reddish material of the 'blood rain' episode on 29-30 May 2013 covered the parking cars and other exposed objects with a thin layer. A stagnant planetary wave determined the synoptic meteorological background of the event and caused the strengthening of blocking Azores and Siberian Highs. The blocked stationary cyclone above Europe diverted an eastward moving 'Sharav' cyclone (developed at the foreside of the Saharan Atlas) into the direction of Central Europe. This event can be classified as a special case of Type-2 events, because the dust transportation was initiated by the 'Sharav' cyclone but later it was diverted by the Central European stationary low-pressure system. The amount of deposited material was ~10-15 $\mu g/m^2$ in Carpathian Basin based on BSC DREAM8b v2.0 model, however, surface observations have pointed to the fact that this value could be underestimated by several orders of magnitudes. Samples were collected from the deposited material and the SEM images showed that some of the quartz particles were exceptionally large; up to 35-40 μm in diameter, however, the majority of mineral grains were smaller (15 μm modal volumetric diameter).

Another event on 19-20 February 2014 was connected to an upper level atmospheric trough as a result of a remarkable meander of the jet stream leading to the development of a cut-off low over NE Africa. With the north-eastwards penetration of the cyclone, dust storms lifted huge amount of mineral dust into the atmosphere which dust-loaded air mass caused an intense washout episode in Hungary (Type-1 Saharan dust event). Laser diffraction-based measurements showed smaller grain size (~6.3 μm modal volumetric diameter) compared to samples collected on 29 May 2013. Similar particle size data is known from previously published studies on Saharan particles collected in Europe (Goudie and Middleton, 2006). However, it is visible on the SEM micrographs that large amounts of particles were transported as medium silt-sized aggregates and could be dispersed during the laser diffraction measurements. Accordingly, the measured particle size results cannot be handled as representative for the wind strength; contrary to the particles gathered during the 2013 episode, when coarse-sized individual particles were identified on the SEM images (Fig. 3.). These assumptions were also confirmed by the automated image analyses of sampled dust material after another intense wet deposition on 19 September 2015. Saharan dust particles were washed out from the north-eastwards penetrating dust laden air-mass (Type-1 dust event). According to backward trajectory calculations and reported surface weather reports, dust material was originated most probably from the Hautes Plaines region of the Atlas Mountains and was transported at the front of a southward moving trough emanating from NW Europe. Mineral particles collected from the deposited material were showing an angular, sub-rounded character with a modal circle-equivalent volumetric diameter of ~20 µm. A large number of aggregates was clearly identifiable on the obtained Malvern Morphologi G3-ID images, suggesting that large proportion of particles were transported not as single grains. It is supposed that, during laser diffraction measurements these sedimentary aggregates would be disintegrated and the obtained grain size distribution would be showing a smaller mean size. On 21 February 2016, a very intense dust outbreak caused severely reduced visibility conditions and remarkable dust deposition in Spain. The dust event was generated again by an atmospheric cut-off low separated from a deepened upper-level through, which low pressure system transported large amounts of the mineral dust northward from salt lakes of high plateau region situated between the Tell Atlas and Saharan Atlas Range (can be classified as a mixture of Type-1 and Type-3 situations). An exceptionally intense wet deposition event was observed on 23 February in Budapest, Hungary, where the deposited reddish-yellow dust material has blanketed parking cars and other exposed obstacles. Granulometric characteristics of collected samples was dominated by clay and fine silt-sized particles (mostly quartz, calcium-carbonate and dolomite), the modal circle-equivalent volumetric diameter of the log-normal grain size distribution was ~10 μm. The value of the granulometric convexity (edge roughness of particles, where higher values indicate smoother particle shapes) of the measured particles was higher compared to the results of event observed on 19 September 2015, indicating a higher individual grain per aggregate ratio. Another unusually intense dust deposition event was observed on 29 February 2016 in Budapest and widespread in the country. The yellowish dust material was transported from Algerian, Tunisian and Libyan source areas at the foreside of a deep cyclone centred above the western basin of Mediterranean Sea (Type-2 Saharan dust event). Particles deposited in the area have a modal circle-equivalent volumetric diameter of ~8 μm with a clear abundance of quartz minerals.

3.2. Modern Saharan dust deposition adjustment based on Mediterranean measurements

Case studies of intense dust deposition events indicated a significant underestimation of surface accumulation provided by numerical models. Similar underestimation was identified in the Mediterranean Basin, where Saharan dust deposition can clearly be documented on islands and in the northern shore of the Mediterranean Sea, even at higher areas where snowpacks contain several brown-pink dust horizons every year (Muhs, 2013). This is also suggested by model calculations by Mahowald et al. (2006), who have reported values between 5 and 10 $g/m^2/y$ for modern dust flux in the investigated area, and most of this dust material originated from the Sahara. Central Europe is situated in the so-called ‘D1b zone’ on the deposition map of Stuut et al. (2009), indicating that this amount of Saharan dust material is playing a role in soil formation by incorporation into the solum and is capable to increase the volumetric concentration of fine-grained mineral fractions.

BSC DREAM8b model comparison with measured surface concentrations and aerosol optical depth showed that the numerical model is able to effectively reproduce the dust cycle (e.g. seasonality patterns, spatial distribution, relative intensity of dust deposition) over North Africa and Europe. However, according to the published Saharan dust deposition measurements, the dust model simulation results were significantly underestimated and showed numerically correct but physically unrealistic low values (Gallisai et al., 2012). Dust deposition values for an extended area can only be estimated by the joint-application of the few, published surface measurements and the underestimated, but spatially-correct model calculations. In-situ field measurements of dust deposition are rare and various techniques have been applied. Reported rates of Saharan dust accumulation in the wider Mediterranean Basin range from 4-5 g/m^2/y up to almost 50 g/m^2/y. By comparing the measured results with modelled values, the simulated results were almost two orders of magnitude lower (Fig. 4.; Table 1). As model evaluations with surface concentration and aerosol optical depth measurements have shown that the numerical simulations were capable to reproduce the dust cycle (e.g. seasonality patterns, spatial distribution), linearly fitted adjustment factors from the Mediterranean can be spatially augmented for a wider European area. The annual simulated deposition rates for the Carpathian Basin (BSC DREAM8b v1.0: 0.0636 g/m^2/y; BSC DREAM8b v2.0: 0.219 g/m^2/y) were multiplied with the weighting scores (BSC DREAM8b v1.0: 95.3709x-2.8614; BSC DREAM8b v2.0: 34.3329x-2.0638) and the goodness-of-fit coefficients (linear correlation coefficients; BSC DREAM8b v1.0: r^2=0.5709; BSC DREAM8b v2.0: r^2=0.853) were applied to estimate the error range. Total annual deposition rates of Saharan dust can be estimated as 5.4±0.81 g/m^2/y (3.17±1.37 g/m^2/y) in the Carpathian Basin according to the adjusted BSC DREAM8b v2.0 (v1.0) results.

3.3. Dust flux values of the Pleistocene interglacials in the Carpathian Basin

Past dust flux estimations are dependent on a reliable chronological framework and sedimentary features of aeolian dust deposits. The local and distant dust material as main sedimentary subpopulations are restored in the bimodal grain size distribution curve and can be decomposed by using mathematical-statistical methods including parametric curve-fitting deconvolution (Sun et al., 2004; Varga et al., 2012) and EMMA end-member modelling algorithms (Weltje, 1997; Weltje and Prins, 2005; Vriend and Prins, 2005). These two populations of aeolian dust deposits are interpreted as the fine-grained continuous background dust-load of the atmosphere and the coarse-grained product of episodic dust storms, by analogy with grain size data of recent dust observations (McTainsh et al., 1997; Sun et al., 2004. The amount of particles of different origin was determined by decomposition of bimodal grain size distributions with parametric curve-fitting method (Fig. 5.). The volumetric fraction of fine-grained component is ranging from 8.9% to 31.8%, but in most cases it is between 10% and 15%. Grain size of this sedimentary population is generally below 20 μm. Very similar grin size data and fine-grained subpopulation proportions were reported by Bokhorst et al., (2011) from other Central European loess sections.

Particle size characteristic of present-day Saharan dust is fairly diverse, but in most cases the dominant component of the transported material is clay and fine silt-sized fraction. Reported grain size values are in the range of 2 to 20-30 μm (data obtained from Goudie and Middleton, 2006): Crete: 8-30 μm (modal – Mattson and Nihlén, 1996), 4-16 μm (median); Spain: 4-30 μm (mean – Sala et al., 1996); Germany: 2.2-16 μm (median); Italy: 16.8 μm (modal), 14.6 µm (median – Ozer et al., 1998); South France: 4-12.7 µm (median – Bücher and Lucas, 1984), 8-11 µm (median – Coudé-Gaussen, 1991); France (Paris Basin): 8 µm (Coudé-Gaussen et al., 1988); Swiss Alps: 4.5±1.5 µm (median – Wagenbach and Geis, 1989); Central Mediterranean: 2-8 µm (modal – Tomadin et al., 1984). These published values and the collected Hungarian samples are very similar to the mathematically separated fine-grained population of interglacial paleosols.

Sedimentation rate [m/y] is expressed as the quotient of loess thickness [m] and duration of loess formation [y], while the dust flux [$g/m^2/y$] is the product of sedimentation rate [m/y] and dry bulk density [kg/m^3]. The calculated total and background dust flux values (by using mass accumulation rates and grain size data) for glacial periods in the Carpathian Basin can be set into the range of 200 to 500 $g/m^2/y$ for total, and 25 to 60 $g/m^2/y$ for background dust deposition, based on loess deposits (Újvári et al., 2010; Varga et al., 2012). It means, Saharan dust could represent a minor addition to the total amount of glacial loess deposits. Újvári et al. (2012) concludes that significant North African contribution to loess deposits is unlikely, although a partial admixture cannot be dismissed according to the Sr-Nd isotope data and a 5 to 10% upper limit can be set as an upper limit on this addition.

During interglacials, the local dust addition is assumed to have ceased (and the loess accumulation was terminated by the soil formation), at the same time the flux of far-travelled Saharan dust material is assessed by the estimated modern values of 3.2 to 5.4 $g/m^2/y$ and remained as a factor of aeolian sedimentation (Fig. 6.). The amount of deposited Saharan dust material can be expressed by the multiplication of interglacial duration and annual Saharan dust flux, however, the determination of duration of soil forming periods is also a challenging problem.

Pleistocene main climatic fluctuations were controlled by the forcing of 100, 41 and 19-23 ky orbital cycles. The superimposition of these harmonic cycles with different wavelength and amplitude creates non-harmonic cycles, clearly visible on reconstructed summer insolation curves. The dominant orbital driver of the various long-term climatic regimes was different from time to time. Precession-determined 19–23 ky Pliocene cyclicity was changed to a dominating obliquity-related 41 ky pattern around two and a half million years ago (onset of the Northern Hemisphere glaciation). The accumulation of the Hungarian loess-paleosol sequences started ~1 My ago, simultaneously with the 100 ky cycles dominance. However, these typical ~100 ky glacial-interglacial variations cannot yet be characterised by homogeneous and equivalent cold and warm fluctuations. Different duration of interglacial periods have long been apparent in paleoclimate records of the Pleistocene (Tzedakis et al., 2012).

The LR04 curve from benthic $\delta^{18}O$ records (Lisiecki and Raymo, 2005) has been used as primary reference curve by Varga (2015) to distinguish odd and even marine isotope stage boundaries. The EPICA DOME C (EDC) δD record was applied to get another independent archive of Middle and Late Pleistocene environmental variations (EPICA Community Members, 2004), and the synthetic Greenland (GLT_syn) record (Barker et al., 2011), calculated from the EPICA record by using the the bipolar-seesaw model was the third reference curve to get a proper global time frame on the global climatic changes. Standardized values of amplitudinal scores were used to define warm (sub-)stages (interglacials and interstadials) as periods with above average mean temperature (Table 2.). For further details of the applied method see Varga (2015).

The total Saharan dust contribution to fine-grained population of soil material is the quotient of deposited Saharan dust material and soil mass of fine-grained population. Assuming that in the Pleistocene interglacials the dust deposition was in the same range as now a days (3.2 to 5.4 $g/m^2/y$), the North African exotic dust material can represent 20-30% of clay and fine silt-sized components in the paleosols (Table 3.).

Calculations based on recent Saharan dust fluxes can be regarded as an average for Late and Middle Pleistocene interglacials, but the amount of emitted North African dust was higher during certain odd marine isotope stages. There are no proxies for past interglacial deposition in the Carpathian Basin, however, some information is available from the Eastern Mediterranean. By correlation of loess-paleosol series from Central Europe with sapropel sequences of the ODP967 marine core (Kroon et al., 1998; Larrasoaña et al., 2003), it is visible that during the formation of the palaeosoils, the Saharan dust flux was fairly weak, similar to the present-day conditions. However, around the Early-Middle Pleistocene transition dust emission from North Africa was also intense during interglacials and there was no sapropel formation in the Eastern Mediterranean. This period overlaps with the formation of red pedogene units in the Carpathian Basin (Marković et al., 2009; 2012). The paleoenvironmental reconstructions and sedimentary data indicated that the formation of Early Pleistocene aeolian deposits was primarily determined by changes in the precipitation patterns rather than by glacial-interglacial variations (Varga, 2011). The climate of the Carpathian Basin in the MIS-19-21 warmer-moist periods was standing more under the influence of the Mediterranean compared to later warm phases, which situation also more likely suggests meridional air-flow patterns and more frequent intrusions of Mediterranean cyclones. Relationship between Saharan dust intrusions and large-scale periodical variations (e.g. El Niño Southern Oscillation, North Atlantic Oscillation) is still controversial. However, intense dust emission periods have been simultaneous with major El Niño events according to Prospero and Lamb (2003). This could be an additional factor in the study of Pliocene red windblown dust deposits (e.g. red clays in the Carpathian Basin), because the time of their formation was determined as the so-called ‘El Padre’ global climate pattern, a permanent El Niño-like state (Ravelo et al., 2006; Shukla el al., 2009).

3.4. Loess-paleosol sequences and syngenetic interglacial dust addition

The possibility of notable interglacial aeolian dust deposition is leading to several questions. According to the classical assumptions for the Carpathian Basin, the glacial loess deposits were formed from the deposited local dust material with a minor addition from distant sources, while the paleosols were developed completely from the underlying loess deposits by weak weathering processes. However, based on the findings of this paper, aeolian dust depositional mechanisms in the Carpathian Basin are more complex. Interglacial dust addition to loess-paleosol sequences and interglacial (and Holocene) loess formation have been reported from several other regions (e.g. Chinese Loess Plateau – Vandenberghe et al., 1997; Prins et al., 2007; Vriend et al., 2011; USA, Alaska – Muhs et al., 2004, 2016; USA, Washington State – Busacca, 1989; Israel – Crouvi et al., 2009), but general characteristics of aeolian dust deposition environment and loess formation of these areas is fairly different from the Central European dust accumulation mechanisms. Saharan dust addition to fine-grained sedimentary subpopulations (3-8 μm) of deposits was identified by Crouvi et al., (2008, 2009) in loess series in the Negev, however major geographic (proximity to Saharan sources) and climatic (warm-arid) conditions of this place are suitable for 'warm loess' formation, while the loess deposits in Central Europe are the products of typical glacial conditions.
Huge amount of stratigraphic and sedimentary data have been published on dust deposition and loess formation of Chinese Loess Plateau. By using the EMMA algorithm, Prins et al., (2007) and Vriend et al., (2011) provided information on background sedimentation and episodic, coarse-grained dust input patterns. These data-sets suggest that the fluxes of glacial and interglacial dust accumulation have been very similar (on average 65 $g/m^2/y$). At the same time, background dust deposition estimations of the present paper are showing firmly different values for glacial and interglacial periods. During glacial periods, the background

dust accumulation based on stratigraphic and sedimentary data can be set into the range of 25 to 60 $g/m^2/y$ as a result of enhanced dust emission from cold-arid European sources and increased Saharan dust fluxes. While the interglacials can be characterised with a ceased dust activity of local and other European source areas, at the same time magnitude and frequency of Saharan dust outbreaks are also reduced during interglacials (Yaalon and Dan, 1974; Tsoar and Pye, 1987).

4. Conclusions

Recent and past Saharan dust mass accumulation in the Carpathian Basin has been assessed in this paper. Estimations derived from the in-situ measurement based adjustment of Saharan dust deposition simulations of BSC DREAM8b v1.0 and v2.0 models indicated that the dust flux of North African fine-grained mineral material can be set into the range of 3.2 to 5.4 $g/m^2/y$. Pleistocene mass accumulation rates calculated from stratigraphic and sedimentary data of loess-paleosol sequences allowed the determination of relative contribution of Saharan dust to interglacial paleosol material. According to these calculations, North African exotic dust material represents 20-30% of the fine-grained component (clay and fine silt-sized fractions) of interglacial paleosols in the Carpathian Basin. The remaining proportion could be regarded as the product of pedogenesis, dust input from additional sources and individual particles remaining after aggregate-disintegration.

The findings from this paper suggest that significant amount of fine-grained Saharan dust was incorporated to interglacial paleosols. This external aeolian dust addition modifies the physicochemical properties of the soils and so, their interpretation in environmental reconstructions. Syngenetic aeolian dust addition has to be taken into account as affecting soil formation of interglacial paleosols. Although the contribution of mineral dust to soils is relatively low, it is capable to modify their fine-grained composition. Geochemical paleoenvironmental proxies derived from clay and fine silt fractions deserve further reconsideration. The fine-grained populations of deposits are consisting of detrital and secondary particles but only secondary ones provide relevant information past environmental conditions. By the assessment of the amount of detrital, windblown particles, the results of reconstructions could be refined significantly.

5. Acknowledgement

Support of the Hungarian Research Fund OTKA under contract PD108708 (for G. Varga) is gratefully acknowledged. It was additionally supported (for G. Varga) by the Bolyai János Research Scholarship of the Hungarian Academy of Sciences.

6. References

Atalay, I., 1997. Red Mediterranean soils in some karstic regions of Taurus mountains, Turkey. Catena 28, 247-260.

Avila, A., Queralt, I., Gallart, F., Martin-Vide, J., 1996. African dust over northeastern Spain: mineralogy and source regions. In: Guerzoni, S. and Chester, R. (Eds.), The impact of desert dust across the Mediterranean. Kluwer, Dordrecht, pp. 201-205.

Barcelona Supercomputing Center's Dust REgional Atmospheric Model Database: http://www.bsc.es/earth-sciences/mineral-dust-forecast-system/

Barker, S., Knorr, G., Edwards, R.L., Parrenin, F., Putnam, A., Skinner, L.C., Wolff, E., Ziegler, M., 2011. 800,000 years of abrupt climate variability. Science 21, 347-351.

Basarin, B., Buggle, B., Hambach, U., Marković, S.B., O'Hara Dhand, K., Kovačević, A., Stevens, T., Guo, Z., Lukić, T., 2014. Time-scale and astronomical forcing of Serbian loess–paleosol sequences. Global Planet. Change 122, 89-106.

Basart, S., Pérez, C., Nickovic, S., Cuevas, E., Baldasano, J.M., 2012. Development and evaluation of the BSC-DREAM8b dust regional model over Northern Africa, the Mediterranean and the Middle East. Tellus B 64, 1-23.

Bergametti, G., Gomes, L., Remoudaki, E., Desbois, M., Martin, D., Buat-Ménard, P., 1989. Present transport and deposition patterns of African dusts to the north-western Mediterranean. In: Leinen, M., Sarnthein, M. (Eds.) Palaeoclimatology and palaeometeorology: modern and past patterns of global atmospheric transport. NATO ASI Ser. C 282, pp. 227-252.

Bokhorst, M.P., Vandenberghe, J., Sümegi, P., Łanczont, M., Gerasimenko, N.P., Matviishina, Z.N., Marković, S.B., Frechen, M., 2011. Atmospheric circulation patterns in central and eastern Europe during the Weichselian Pleniglacial inferred from loess grain-size records. Quatern. Int. 234, 62-74.

Bronger, A., 2003. Correlation of loess–paleosol sequences in East and Central Asia with SE Central Europe: towards a continental Quaternary pedostratigraphy and paleoclimatic history. Quatern. Int.106-107, 11-31.

Bücher, A., Lucas, G., 1984. Sédimentation éolienne intercontinentale, poussières sahariennes et géologie. Bull. Cent. Rech. Elf. E. 8, 151-165.

Buggle, B., Hambach, U., Müller, K., Zöller, L., Marković, S.B., Glaser, B., 2014. Iron mineralogical proxies and Quaternary climate change in SE-European loess–paleosol sequences. Catena 117, 4-22.

Busacca, A.J., 1989. Long Quaternary record in Eastern Washington, U.S.A., interpreted from multiple buried paleosols in loess. Geoderma 45, 105-122.

Crouvi, O., Amit, R., Enzel, Y., Sandler, A., 2008. Sand dunes as a major proximal dust source for Late Pleistocene loess in the Negev Desert, Israel. Quaternary Res. 70, 275-282.

Crouvi, O., Amit, R., Porat, N., Gillespie, A.R., McDonald, E.V., Enzel, Y., 2009. Significance of promary hilltop loess in reconstructing dust chronology, accretion rates and sources: An example from the Negev Desert, Israel. J. Geophys. Res. 114, F02017, DOI : 10.1029/2008JF001083

Coudé-Gaussen, G., 1991. Les poussières sahariennes: cycle sédimentaire et place dans les environments et paléoenvironments désertiques. Montrouge: John Libby Eurotext, 485 pp.

Coudé-Gaussen, G., Désiré, E., Regrain, R., 1988. Particularité de poussières sahariennes distales tombées sur la Picardie et l'Ile-de-France le 7 Mai 1988. Hommes Terr. N. 4, 246-251.

Draxler, R.R., Hess, G.D., 1997. Description of the HYSPLIT_4 modeling system. NOAA Tech. Memo. ERL ARL-224, NOAA Air Resources Laboratory, Silver Spring, MD, 24 p.

Draxler, R.R., Rolph, G.D., 2012. HYSPLIT (HYbrid Single-Particle Lagrangian Integrated Trajectory) Model access via NOAA ARL READY Website (http://ready.arl.noaa.gov/HYSPLIT.php). NOAA Air Resources Laboratory, Silver Spring, MD.

Durn, G., Ottner, F., Slovenec, D., 1999. Mineralogical and geochemical indicators of the polygenetic nature of terra rossa in Istria, Croatia. Geoderma 91, 125-150.

Durn, G., 2003. Terra rossa in the Mediterranean Region: Parent materials, composition and origin. Geol. Croat. 56, 83-100.

EPICA Community Members, 2004. Eight glacial cycles from an Antarctic ice core. Nature 429, 623-628.

Fiol, L.A., Fornós, J.J., Gelabert, B., Guijarro, J.A., 2005. Dust rains in Mallorca (Western Mediterranean): their occurrence and role in some recent geological processes. Catena 63, 64-84.

Gábris, Gy., 2007. The relation between the time scale of the Quaternary surface processes and oxygen isotope stratigraphy – according to the loess–palaeosoil sequences and river terraces in Hungary. Földt. Közl. 137, 515-540.

Gallisai, R., Peters, F., Basart, S., Baldasano, J.M., 2012. Mediterranean basin-wide correlations between Saharan dust deposition and ocean chlorophyll concentration. Biogeosciences Discuss. 9, 8611-8639.

Genova, N., Meloni, S., Oddone, M., Melis, P., 2001. On the origin of some red soils from Sardinia (Italy): A neutron activation analysis investigation. Journal of Radioanal. Nucl. Ch. 249, 355-360.

Goudie, A.S., Middleton, N.J., 2001. Saharan dust storms: Nature and consequences, Earth-Sci. Rev. 56, 179-204.

Goudie, A.S., Middleton, N.J., 2006. Desert Dust in the Global System. Springer, 287 p.

Harrison, S.P., Kohfeld, K.E., Roelandt, C., Claquin, T., 2001. The role of dust in climate changes today, at the last glacial maximum and in the future. Earth-Sci. Rev. 54, 43-80.

Herut, B., Krom, M., 1996. Atmospheric input of nutrients and dust to the SE Mediterranean. In: Guerzoni, S., Chester, R. (Eds.) The impact of desert dust across the Mediterranean. Kluwer, Dordrecht, pp. 349-358

Horváth, E., Bradák, B., 2014. Sárga föld, lősz, lösz: Short historical overview of loess research and lithostratigraphy in Hungary. Quatern. Int. 319, 1-10.

Israelevich, P.L., Levin, Z., Joseph, J.H., Ganor, E., 2002. Desert aerosol transport in the Mediterranean region inferred from the TOMS aeosol index. J. Geophys. Res-Atmos 107 (D21) DOI: 10.1029/2001JD002011

Jackson, M.L., Clayton, R.N., Violante, A., Violante, P., 1982. Eolian influence on terra rossa soils of Italy traced by quartz oxygen isotopic ratio. In: van Olphen, H., Veniale, F., (Eds.) International Clay Conference, Bologna and Pavia, Italy, September 1981, Elsevier, Amsterdam, pp. 293-300.

Jahn, R., Zarei, M., Stahr, K., 1991. Genetic implications of quartz in “Terra Rossa”-soils in Portugal. Proceedings of 7th Euroclay Conference, Dresden, pp. 541-546.

Jordanova, D., Hus, J., Evgoljev, J., Geeraerts, R., 2008. Paleomagnetism of the loess /paleosol sequence in Viatovo (NE Bulgaria) in the Danube Basin. Phys. Earth Planet. Inter. 167, 71-83.

Jordanova, N., Jordanova, D., Liu, Q., Hu, P., Petrov, P., Petrovský, E., 2013. Soil formation and mineralogy of a Rhodic Luvisol — insights from magnetic and geochemical studies. Global Planet. Change 110, 397-413.

Kalnay, E., Kanamitsu, M., Kistler, R., Collins, W., Deaven, D., Gandin, L., Iredell, M., Saha, S., White, G., Woollen, J., Zhu, Y., Leetmaa, A., Reynolds, B., Chelliah, M., Ebisuzaki, W., Higgins, W., Janowiak, J., Mo, K. C., Ropelewski, C., Wang, J., Jenne, R., Joseph, D., 1996. The NCEP/NCAR 40-Year Reanalysis Project. B. Am. Meteorol. Soc. 77, 437-471.

Kohfeld, K.E., Tegen, I., 2007. Record of Mineral Aerosols and Their Role in the Earth System. Treatise on Geochemistry 4, pp. 1-26.

Konert, M., Vandenberghe, J., 1997. Comparison of laser grain-size analysis with pipette and sieve analysis: a solution for the underestimation of the clay fraction. Sedimentology 44, 523-535.

Kovács J., 2008. Grain-size analysis of the Neogene red clay formation in the Pannonian Basin. Int. J. Earth Sci. 97, 171-178.

Kovács, J., Varga, Gy., Dezső, J., 2008. Comparative study on the Late Cenozoic red clay deposits from China and Central Europe (Hungary). Geol. Q. 52, 369-382.

Kovács, J., Fábián, S.T., Varga, G., Újvári, G., Varga, G., Dezső, J. 2011. Plio-Pleistocene red clay deposits in the Pannonian basin: A review. Quatern. Int. 240, 35-43.

Kovács, J., Raucsik, B., Varga, A., Újvári, G., Varga, Gy., Ottner, F., 2013. Clay mineralogy of red clay deposits from the Central Carpathian Basin (Hungary): Implications for Plio/Pleistocene chemical weathering and paleoclimate. Turk. Jour. Earth Sci. 22, 414-426.

Kubiëna, W.L., 1953. The soils of Europe: illustrated diagnosis and systematics. Murby, London 317 p.

Le-Bolloch, O., Guerzoni, S., Molinaroli, E., 1996. Atmosphere-ocean mass fluxes at two coastal sites in Sardinia 39-41 degrees N, 8-10 degrees E. In: Guerzoni, S., Chester, R. (Eds.) The impact of desert dust across the Mediterranean. Kluwer, Dordrecht, pp. 217-222.

Leiningen, W. Graf zu, 1915. Ueber die Einflüsse von äolischer Zufuhr auf die Bodenbil-dung. Mitteilungen der Geologischen Gesellschaft in Wien Bd. VIII, S. 139-177.

Leiningen, W., Graf zu, 1930. Die Roterde (Terra Rossa), Lösungsrest mariner Kalksteine. Chemie der Erde 4, 178-187.

Lisiecki, L., Raymo, M.E., 2005. A Pliocene–Pleistocene stack of 57 globally distributed benthic δ18O records. Paleoceanography 20, PA1003. DOI: 10.1029/2004PA001071

Loÿe-Pilot, M.D., Martin, J.M., Morelli, J., 1986. Influence of Saharan dust on the rain acidity and atmospheric input to the Mediterranean. Nature 321, 427-428.

MacLeod, D.A., 1980. The origin of the red Mediterranean soils in Epirus, Greece. J. Soil Sci. 31, 125-136.

Maher, B.A., Prospero, J.M., Mackie, D., Gaiero, D., Hesse, P.P., Balkanski, Y., 2010. Global connenctions between aeolian dust, climate and ocean biogeochemistry at the present day and at the last glacial maximum. Earth-Sci. Rev. 99, 61-97.

Marković, S.B., Hambach, U., Catto, N., Jovanović, M., Buggle, B., Machalett, B., Zöller, L., Glaser, B., Frechen, M., 2009. Middle and Late Pleistocene loess sequences at Batajnica, Vojvodina, Serbia. Quatern. Int. 198, 255-266.

Marković, S.B., Hambach, U., Stevens, T., Kukla, G.J., Heller, F., McCoy, W.D., Oches, E.A., Buggle, B., Zöller, L., 2011. The last million years recorded at the Stari Slankamen (Northern Serbia) loess-palaeosol sequence: revised chronostratigraphy and long-term environmental trends. Quaternary Sci. Rev. 30, 1142-1154.

Marković, S.B., Hambach, U., Stevens, T., Jovanović, M., O'Hara-Dhand, K., Basarin, B., Lu, H., Smalley, I.J., Buggle, B., Zech, M., Svirčev, Z., Sümegi, P., Milojković, N., Zöller, L., 2012. Loess in the Vojvodina region (Northern Serbia): an essential link between European and Asian Pleistocene environments. Neth. J. Geosci. 91, 173-188.

Marković, S.B., Stevens, T., Kukla, G.J., Hambach, U., Fitzsimmons, K.E., Gibbard, P., Buggle, B., Zech, M., Guo, Z., Hao, Q., Wu, H., O'Hara Dhand, K., Smalley, I.J., Újvári, G., Sümegi, P., Timar-Gabor, A., Veres, D., Sirocko, F., Vasiljević, D.A., Jary, Z., Svensson, A., Jović, V., Lehmkuhl, F., Kovács, J., Svirčev, Z., 2015. Danube loess stratigraphy — Towards a pan-European loess stratigraphic model. Earth-Sci. Rev. 148, 228-258.

Mattsson, J.O., Nihlén, T., 1996. The transport of Saharan dust to southern Europe: a scenario. J. Arid Environ. 32, 111-119.

McTainsh, G.H., Nickling, W.G., Lynch, A.W., 1997. Dust deposition and particle size in Mali, West Africa. Catena 29, 307-322.

Moulin, C., Lambert, C.E., Dayan, U., Masson, V., Ramonet, M., Bousquet, P., Legrand, M., Balkanski, Y.I., Guelle, W., Marticorena, B., Bergametti, G., Dulac, F., 1998. Satellite climatology of African dust transport in the Mediterranean atmosphere. J. Geophys. Res. 103, 13137-13144.

Muhs, D.R., McGeehin, J.P., Beann, J., Fisher, E., 2004. Holocene loess deposition and soil formation as competing processes, Matanuska Valley, southern Alaska. Quaternary Res. 61, 265-276.

Muhs, D.R., Budahn, J., Avila, A., Skipp, G., Freeman, J., Patterson, DeA., 2010. The role of African dust in the formation of Quaternary soils on Mallorca, Spain and implications for the genesis of Red Mediterranean soils. Quaternary Sci. Rev. 29, 2518-2543.

Muhs, D.R., 2013. The geologic records of dust in the Quaternary. Aeol. Res. 9, 3-48.

Muhs, D.R., Budahn, J.R., Skipp, G.L., McGeehin, J.P., 2016. Geochemical evidence for seasonal controls on the transportation of Holocene loess, Matanuska Valley, southern Alaska, USA. Aeol. Res. 21, 61-73.

Nihlén, T., Mattsson, J.O., 1989. Studies on eolian dust in Greece. Geogr. Ann. 71, 269-274.

Nihlén, T., Olsson, S., 1995. Influence of eolian dust on soil formation in the Aegean area. Z. Geomorphol. 39, 341-361.

Novothny, Á., Frechen, M., Horváth, E., Wacha, L., Rolf, C., 2011. Investigating the penultimate and last glacial cycles of the Süttő loess section (Hungary) using luminescence dating, high-resolution grain size, and magnetic susceptibility data. Quatern Int. 234, 75-85.

Ozer, P., Erpicum, M., Cortemiglia, G.C., Lucchetti, G., 1998. A dustfall event in November 1996 in Genoa, Italy. Weather 53, 140-145.

Pécsi, M., 1990. Loess is not just the accumulation of dust. Quatern. Int. 7-8. 1-21.

Pécsi, M., Schweitzer, F., 1995. The lithostratigraphical, chronostratigraphical sequence of Hungarian loess profiles and their geomorphological position. In: Pécsi, M., Schweitzer, F. (eds.): Loess InForm 3. Concept of loess, loess-paleosol stratigraphy. MTA FKI, Budapest: 31-61.

Pérez, C., Nickovic, S., Baldasano, J. M., Sicard, M., Rocadenbosch, F., Cachorro, V. E., 2006a. A long Saharan dust event over the western Mediterranean: Lidar, Sun photometer observations, and regional dust modeling. J. Geophys. Res. Atmos. 111, D15214, doi:10.1029/2005JD006579

Pérez, C., Nickovic, S., Pejanovic, G., Baldasano, J.M., Özsoy, E., 2006b. Interactive dust-radiation modeling: A step to improve weather forecasts. J. Geophys. Res. Atmos. 111, D16206, doi:10.1029/2005JD006717

Prins, M.A., Vriend, M., Nugteren, G., Vandenberghe, J., Lu, H., Zheng, H., Weltje, G.J., 2007. Late Quaternary aeolian input variability on the Chinese Loess Plateau: inferences from unmixing of loess grain-size records. Quaternary Sci. Rev. 26, 230-242.

Pye, K., 1987. Aeolian Dust and Dust Deposits. Academic Press, London, 334 p.

Pye, K., 1995. The nature, origin and accumulation of loess. Quaternary Sci. Rev. 14, 653-667.

Rapp, A., 1983. Are Terra rossa soils in Europe eolian deposits from Africa? Geol. Foren. Stock. For. 105, 161-168.

Sala, J.Q., Cantos, J.O., Chiva, E.M., 1996. Red dust within the Spanish Mediterranean area. Clim. Change 32, 215-228.

Sartori, M., Heller, F., Forster, T., Borkovec, M., Hammann, J., Vincent, E., 1999. Magnetic properties of loess grain size fractions from the section at Paks (Hungary). Phys. Earth Planet In. 116, 53-64.

Stuut, J-B.W., Smalley, I., O'Hara-Dhand, K., 2009. Aeolian dust in Europe: African sources and European deposits. Quatern. Int. 198, 234-245.

Sun, D., Bloemendal, J., Rea, D.K., An, Z., Vandenberghe, J., Lu, H., Su, R., Liu, T.S., 2004. Bimodal grain-size distribution of Chinese loess, and its paleoclimatic implications. Catena 55, 325-340.

Ternon, E., Guieu, C., Loÿe-Pilot, M-D., Leblond, N., Bosc, E., Gasser, B., Miquel, J.-C., Martin, 2010. The impact of Saharan dust on the particulate export in the water column of the North Western Mediterranean Sea. Biogeosciences 7, 809-826.

Tomadin, L., Lenaz, R., Landuzzi, V., Mazzucoletti, A., Vannucci, R. 1984. Wind-blown dust over the central Mediterranean. Oceanol. Acta 7, 13-23.

Tsoar, H., Pye, K., 1987. Dust transport and the question of desert loess formation. Sedimentology 34, 134-153.

Tzedakis, P.C., Wolff, E.W., Skinner, L.C., Brovki, V., Hodell, D.A., McManus, J.F., Raynaud, D. 2012. Can we predict the duration of an interglacial? Clim. Past 8, 1473-1485.

Újvári, G., Kovács, J., Varga, Gy., Raucsik, B., Marković, S.B., 2010. Dust flux estimates for the Last Glacial Period in East Central Europe based on terrestrial records of loess deposits: a review. Quaternary Sci. Rev. 29, 3157-3166.

Újvári, G., Varga, A., Ramos, F.C., Kovács, J., Németh, T., Stevens, T., 2012. Evaluating the use of clay mineralogy, Sr-Nd isotopes and zircon U-Pb ages in tracking dust provenance: an example from loess of the Carpathian Basin. Chem. Geol. 304-305, 83-96.

Újvári, G., Varga, A., Raucsik, B., Kovács, J., 2014. The Paks loess-paleosol sequence: A record of chemical weathering and provenance for the last 800 ka in the mid-Carpathian Basin. Quatern. Int. 319, 22-37.

Vandenberghe, J., An, Z., Nugteren, G., Lu, H., Van Huissteden, J., 1997. New absolute time scale for the Quaternary climate in the Chinese loess region by grain-size analysis. Geology 25, 35-38.

Vandenberghe, J., 2013. Grain size of fine-grained windblown sediment: A powerful proxy for process identification. Earth-Sci. Rev. 121, 18-30.

Vandenberghe, J., Markovič, S.B., Jovanovič, M., Hambach, U., 2014. Site-specific variability of loess and palaeosols (Ruma, Vojvodina, northern Serbia). Quatern. Int., 334-335, 86-93.

Varga, Gy., 2011. Similarities among the Plio–Pleistocene terrestrial aeolian dust deposits in the World and in Hungary. Quatern. Int. 234, 98-108.

Varga, Gy., Kovács, J., Újvári, G., 2012. Late Pleistocene variations of the background aeolian dust concentration in the Carpathian Basin: an estimate using decomposition of grain-size distribution curves of loess deposits. Neth. J. Geosci. 91, 159-171.

Varga, Gy., Kovács, J., Újvári, G., 2013 Analysis of Saharan dust intrusions into the Carpathian Basin (Central Europe) over the period of 1979-2011. Global Planet. Change 100, 333-342.

Varga, Gy., Újvári, G., Kovács, J., 2014a. Spatiotemporal patterns of Saharan dust outbreaks in the Mediterranean Basin. Aeol. Res. 15, 151-160.

Varga, Gy., Cserháti Cs., Kovács, J., Szeberényi, J., Bradák, B., 2014b. Unusual Saharan dust events in the Central European Carpathian Basin in 2013 and early 2014. Weather 69, 309-313.

Varga, Gy., 2015. Changing nature of pleistocene interglacials – is it recorded by paleosoils in Hungary (Central Europe)? Hung Geogr Bull 64, 313–322.

Vriend, M., Prins, M.A., 2005. Calibration of modelled mixing patterns in loess grain-size distributions: an example from the north-eastern margin of the Tibetan Plateau, China. Sedimentology 52, 1361.1374.

Vriend, M., Prins, M.A., Buylaert, J.-P., Vandenberghe, J., Lu, H., 2011. Contrasting dust supply patterns across the north-western Chinese Loess Plateau during the last glacial-interglacial cycle. Quatern. Int. 240, 167-180.

Wagenbach, D., Geis, K., 1989. The mineral dust record in a high alpine glacier (Colle Gnifett, Swiss Alps). In: Leinen, M., Sarnthein, M. (Eds.) Paleoclimatology and paleometeorology: modern and past patterns of global atmospheric transport. Kluwer, Dordrecht, pp. 543-564

Weltje, G.J., 1997. End-member modeling of compositional data: numerical–statistical algorithms for solving the explicit mixing problem. J. Math. Geol. 29, 503-549.

Weltje, G.J., Prins, M.A. 2007. Genetically meaningful decomposition of grain-size distributions. Sediment. Geol. 202, 409-424.

Yaalon, D.H., 1997: Soils in the Mediterranean region: what makes them different? Catena. 28, 157-169.

Yaalon, D.H., Ganor, E., 1973. The influence of dust on soils during the Quaternary. Soil Sci. 116, 146-155.

Yaalon, D.H., Dan, J., 1974. Accumulation and distribution of loess-derived deposits in the semi-arid desert fringe area of Israel. Z. Geomorphol. Supp. 20, 91-105.

Table 1. Model simulation results and in-situ measurements of Saharan dust deposition in the wider Mediterranean Basin.

Site		Deposition [g/m²/y]							
		BSC DREAM8b v1.0			BSC DREAM8b v2.0			Measurement	
		Dry	Wet	Total	Dry	Wet	Total	Total	References
a	Central France	0.03	0.04	0.07	0.04	0.08	0.12	1	Bücher and Lucas (1984)
b	NE Spain (Montseny)	0.09	0.08	0.17	0.14	0.13	0.27	5.2 (5.1–5.3)	Avila et al. (1996)
c	Mallorca	0.04	0.07	0.11	0.17	0.13	0.30	4.5	Fiol et al. (2005)
d	Ligurian Sea	0.02	0.06	0.08	0.09	0.16	0.25	11.4	Ternon et al. (2010)
e	Corsica	0.06	0.12	0.18	0.13	0.23	0.37	12	Bergametti et al. (1989)
f	Corsica	0.06	0.12	0.18	0.13	0.23	0.37	12.5	Löye-Pilot et al. (1986)
g	S Sardinia	0.09	0.12	0.21	0.30	0.27	0.57	9.5 (6–13)	Le-Bolloch et al. (1996)
h	Aegean Sea	0.06	0.09	0.15	0.27	0.29	0.56	23.9 (11.2–36.5)	Nihlén and Olsson (1995)
i	Crete	0.22	0.12	0.34	0.54	0.31	0.85	26 (6–46)	Nihlén and Mattsson (1989)
j	SE Mediterranean	0.21	0.09	0.30	0.78	0.29	1.08	36	Herut and Krom (1996)

Table 2. Estimated duration of interglacials in thousand years, based on Varga, 2015. Data series of the following reference curves have been used in our calculations: LR04 benthic stack: it is an average of 57 globally distributed benthic $\delta^{18}O$ records (Lisiecki and Raymo

2005); EDC: EPICA DOME C ice core record [δD] (EPICA Community Members 2004); GLT_syn: synthetic Greenland $\delta^{18}O$ record, constructed from the EDC record based on the bipolar-seesaw model (Barker et al., 2011).

Stage	LR04 benthic $\delta^{18}O$ stack [ky]			EPICA DOME C ice core record [ky]			GLT_syn: synthetic Greenland $\delta^{18}O$ record [ky]		
	End	Start	Duration	End	Start	Duration	End	Start	Duration
MIS-5a	81	85	4	–	–	–	–	–	–
MIS-5c	94	101	7	–	–	–	–	–	–
MIS-5e	114	132	18	114	134	20	114	130	16
MIS-7c	206	219	13	206	218	12	204	215	11
MIS-7e	234	244	10	237	246	9	234	243	9
MIS-9e	318	336	18	322	338	16	320	335	15
MIS-11c	395	421	26	391	425	34	391	426	35
MIS-13a	484	503	19	482	499	17	481	499	18
MIS-15a	572	581	9	564	580	16	560	580	20
MIS-15c	604	618	14	603	623	20	604	626	22
MIS-17	690	704	14	688	707	19	686	703	17
MIS-19c	772	790	18	773	786	13	773	789	16
MIS-21c	838	866	28	–	–	–	–	–	–

Table 3. Estimated Saharan dust contribution to fine-grained fractions of paleosoils.

Paleosoil ID	Age	Estimated duration of soil formation [ky]	Thickness [cm][4]	Fine-grained component [%][5]	Soil mass [kg][6]		Saharan dust contribution [kg]			Saharan contribution [%][7]
					Total	Fine-grained	v1.0	v2.0	Mean	
MF2_1[1]	MIS-5a	4.0	50	8.9	900	80.2	12.7	21.6	17.1	21.4
MF2_2[1]	MIS-5c	7.0	50	14.7	900	132.2	22.2	37.8	30.0	22.7
MF2_3[1]	MIS-5e	18.0	80	13.2	1440	189.9	57.1	97.2	77.1	40.6
BD1	MIS-7c	12.0	80	13.0	1440	187.0	38.0	64.8	51.4	27.5
BD2	MIS-7e	9.3	60	11.9	1080	128.1	29.6	50.4	40.0	31.2
BA	MIS-9e	16.3	110	15.7	1980	309.9	51.8	88.2	70.0	22.6
MB	MIS-11c	31.7	140	31.8	2520	801.5	100.4	171.0	135.7	16.9
Phe1[2]	MIS-13a	18.0					57.1	97.2	77.1	
Phe2[2]	MIS-15a	15.0					47.6	81.0	64.3	
Mtp1[2]	MIS-15c	18.7					59.2	100.8	80.0	
Mtp2[2]	MIS-17	16.7					52.8	90.0	71.4	
PD1[3]	MIS-19	29.0	210	14.6	3780	551.0	91.9	156.6	124.3	22.6
PD2	MIS-21c	28.0	180	14.0	3240	454.6	88.8	151.2	120.0	26.4

[1] As MF2 soils cannot be identified in the investigated Paks section, samples were taken from the Tamási section (Hungary).
[2] Correlation of these units with MIS-13 and MIS-15 stages is uncertain and the thickness of soils is underestimated due to proposed stratigraphic hiatuses.
[3] Calculations were performed for the whole MIS-19 stage.
[4] Soil thickness can change from section to section, these numbers can be regarded as tentative, mean values.
[5] Clay- and fine silt-sized fraction of the soil (proportion estimated by parametric curve-fitting).
[6] A dry density value of 1.8 g/cm^3 were employed for calculations of volume of soil column with 1 m^2 base.
[7] Estimation of Saharan dust contribution to the fine-grained soil components in percent.

Figure captions

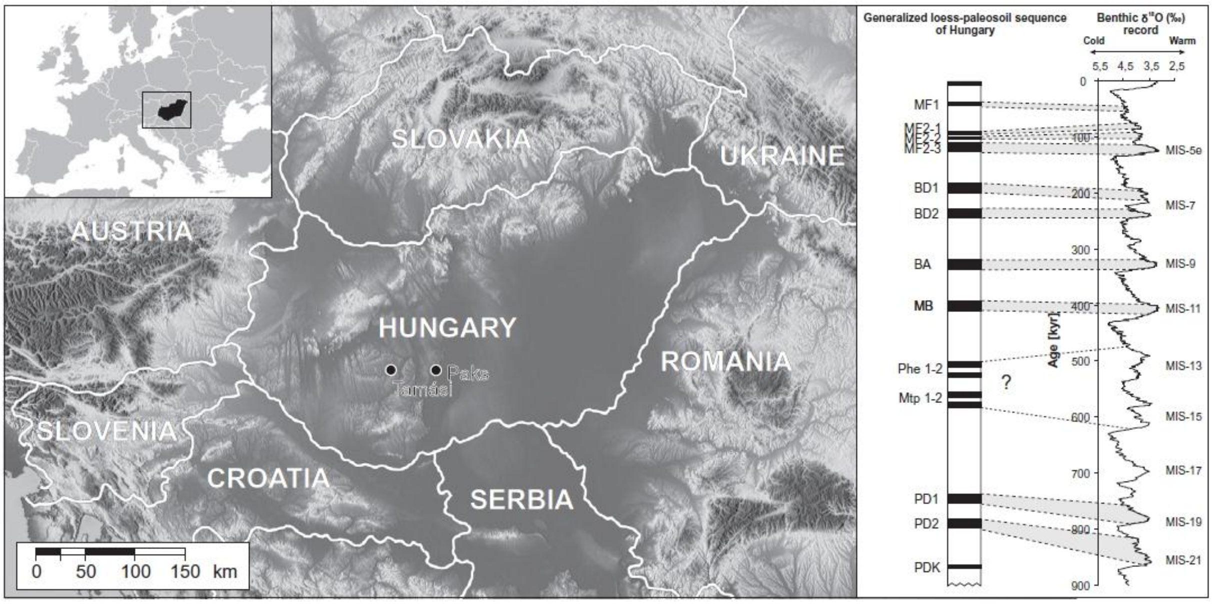

Figure 1. Investigated area and generalized loess-paleosoil sequence of Hungary with its possible correlation with benthic $\delta^{18}O$ record of deep sea sediments (Lisiecki and Raymo, 2005).

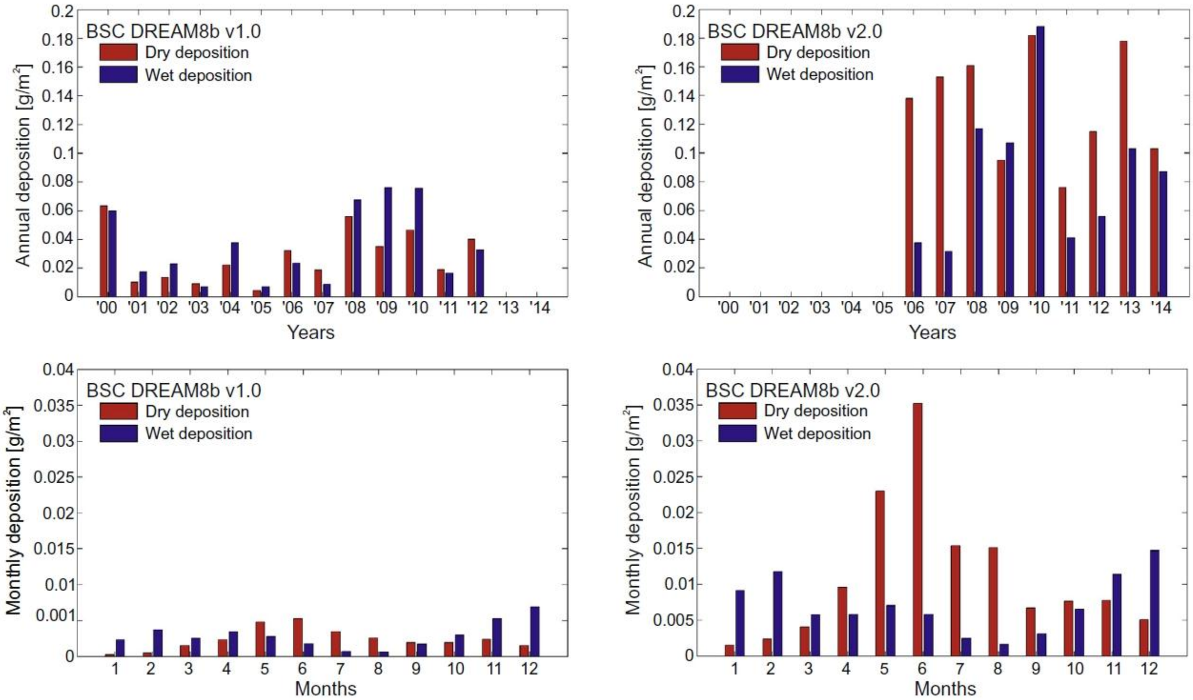

Figure 2. Interannual and seasonal distribution of dry and wet Saharan dust deposition in the Carpathian Basin.

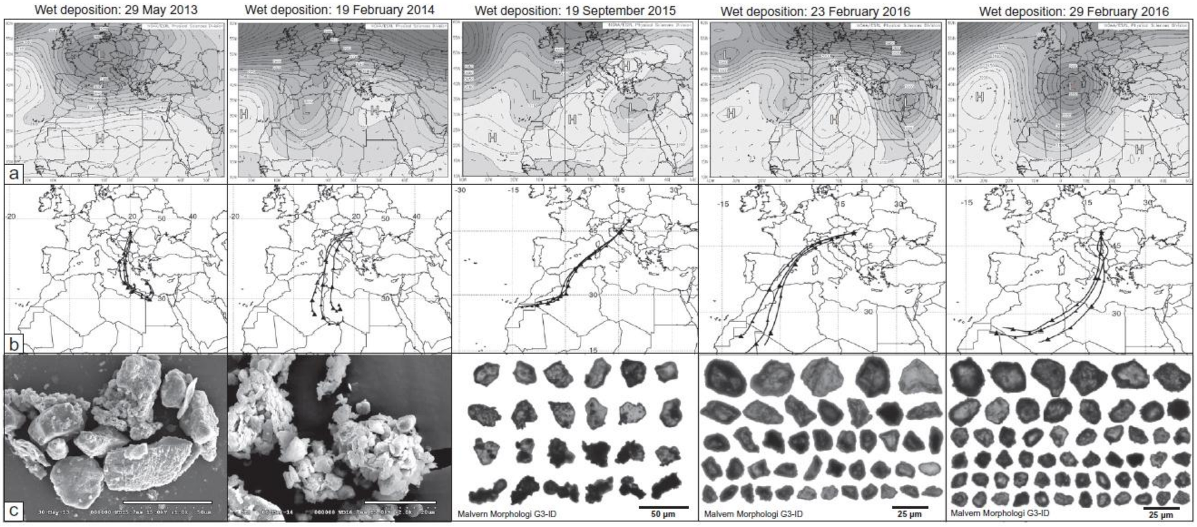

Figure 3. Intense Saharan dust depositional events in the Carpathian Basin (a: mean geopotential height and wind vectors at 700 hPa during the SDEs; b: trajectories of Saharan dust transportation; c: SEM micrographs and Malvern Morphologi G3-ID images of collected dust samples).

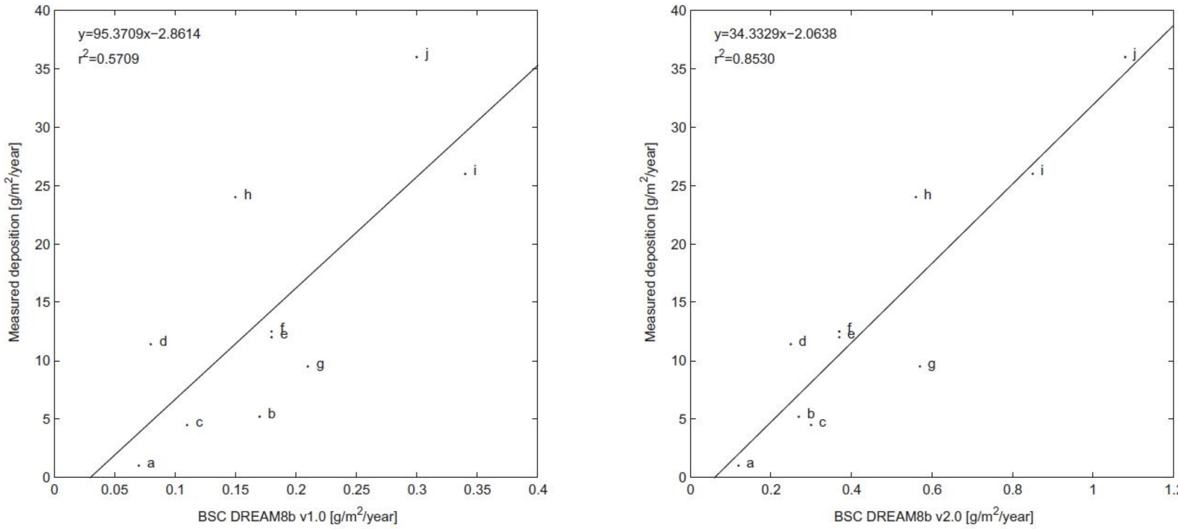

Figure 4. Comparison of modelled and measured Saharan dust deposition values at different sites (for abbreviations see Table 1).

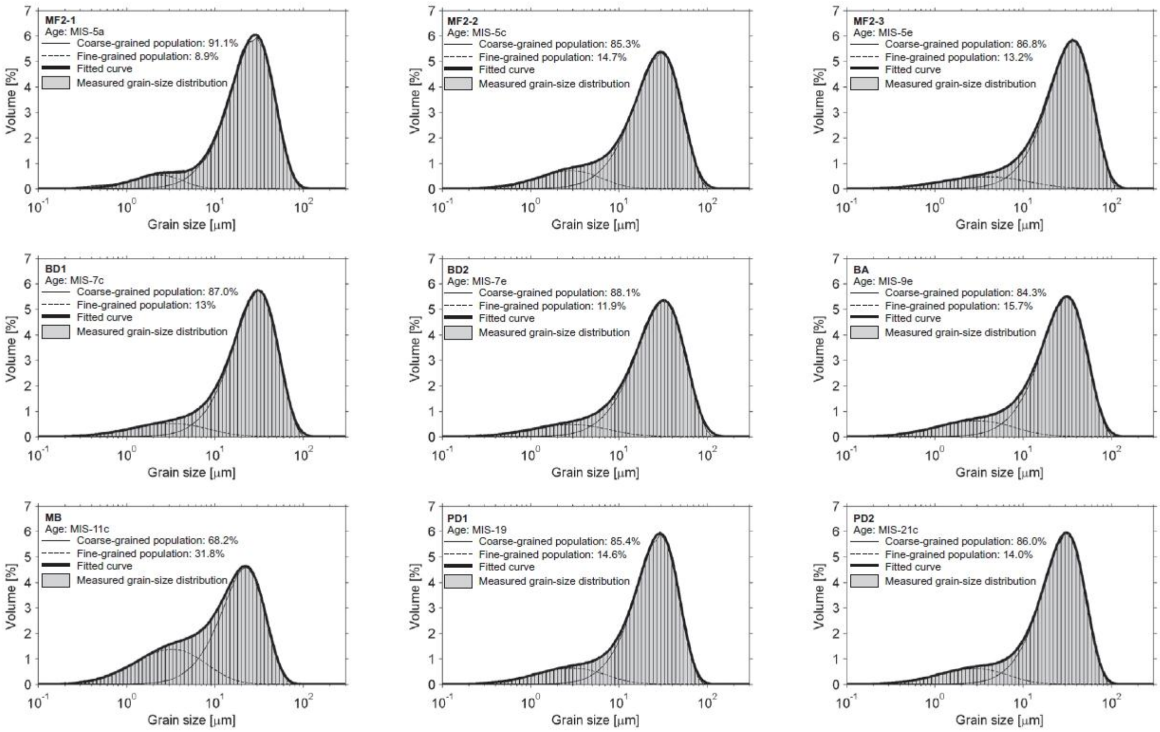

Figure 5. Grain size distribution curves of interglacial paleosoils and results of mathematical-statistical separation of sediment populations via parametric curve-fitting method.

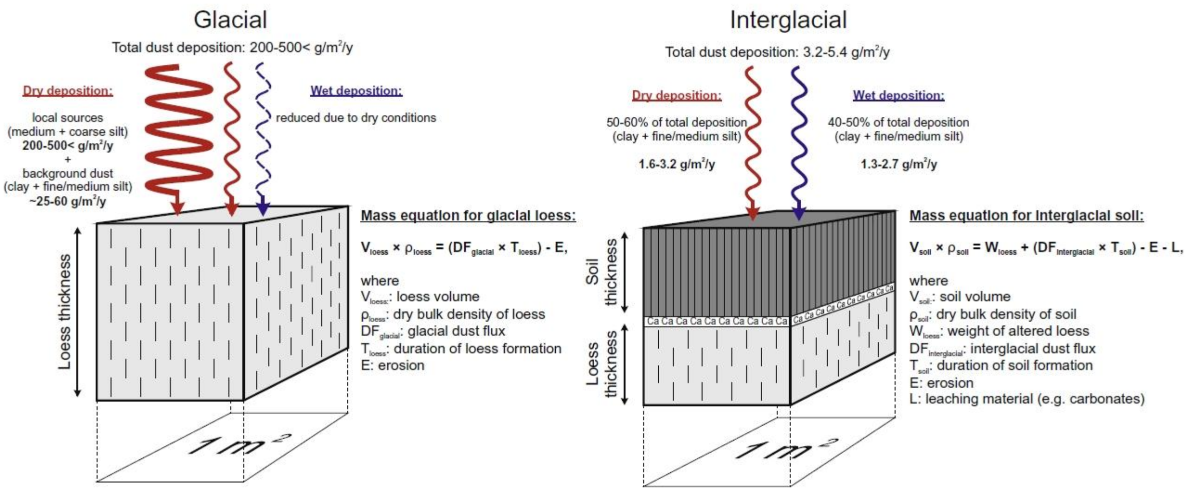

Figure 6. Schematic illustration of glacial and interglacial dust deposition mechanisms.